

# On the Excitation of Double Giant Resonances in Heavy Ion Reactions

C.H. Dasso <sup>a</sup>, L. Fortunato <sup>b</sup>, E. G. Lanza <sup>c</sup> and A. Vitturi <sup>b</sup>

<sup>a</sup>*Departamento de Física Atómica, Molecular y Nuclear,  
Universidad de Sevilla, Spain*

<sup>b</sup>*Dipartimento di Fisica “G.Galilei”, Università di Padova and INFN, Italy*

<sup>c</sup>*INFN-Catania and Dipartimento di Fisica e Astronomia,  
Università di Catania, Italy*

---

## Abstract

The interplay of nuclear and Coulomb processes in the inelastic excitation of single- and double-phonon giant resonances in heavy ion collisions is studied within a simple reaction model. Predominance of the Coulomb excitation mechanism on the population of the single-phonon and, on the contrary, predominance of the nuclear excitation for the double-phonon is evidenced. The effect of the spreading of the strength distribution of the giant resonances on the excitation process is analyzed, showing sizeable modifications in the case of Coulomb dominated processes.

*Key words:* Multiphonon collective excitation, Double Giant Resonance, Spreading width.

*PACS:* 24.30.Cz, 25.70.-z, 25.70.De

---

## 1 Introduction.

Giant Resonances (GR) are considered as one of the most important elementary modes of excitation in nuclei (1). They are generally interpreted as harmonic density vibrations around the equilibrium distribution of the nucleons. Within this point of view one should also expect to observe higher-lying states of the harmonic spectrum such as, for instance, the two-phonon Double Giant Resonance (DGR). The existence of the double-phonon excitation of low-lying collective vibrational states has been known for a long time, but it is only recently that the multiple excitations of GR have been systematically observed (for a complete review see ref.(2) and (1) and references therein).

Interest in this subject has been renewed by recent experiments with relativistic heavy-ion beams, where inelastic cross sections for the excitation of the dipole DGR have been precisely measured. The theoretically calculated cross sections – when performed within the framework of the standard harmonic model – systematically underestimate the experimental data by as much as a factor of two. This unexpected enhancement of the cross sections puts in evidence shortcomings in either the description of the structure of the modes or in the formulation of the reaction mechanism. Attempts to improve over this situation have followed different paths.

The microscopic understanding of these resonances, for instance, has been taken beyond the simple superposition of the 1p-1h configurations to include couplings to 2p-2h, 3p-3h and/or states of higher complexity (3; 4; 5). Residual interactions give rise to anharmonicity in the energy spectrum (6) and, also, appreciable changes in the structure of the wave functions. Recently, a systematic study of the anharmonicity in the dipole DGR has been carried out for several nuclei (7). This study, based on a quasiparticle RPA, has shown an effect of few hundred keV. The same order of magnitude had been found in ref. (8) for  $^{208}\text{Pb}$  and  $^{40}\text{Ca}$ . These effects have been taken into account in macroscopic models that add small anharmonic contributions (9; 10) to the otherwise harmonic hamiltonian in the presence of an external time-dependent field. Depending on the magnitude of these anharmonic terms the inelastic cross sections for the population of the dipole DGR can reach values which are close to the experimental data. Microscopic calculations in the context of the RPA approximation, have also succeeded in reducing the discrepancy between the experimental data and the theoretical predictions down to the level of a few per cent (8). Another approach to the problem that has been examined (12; 13) exploits the so-called Brink-Axel hypothesis (11). It also seems possible, through this formalism, to obtain enhancements in the population of states in the energy range around the DGR.

In this paper we set to investigate the role of the nuclear coupling in the excitation of GR's and DGR's and its interplay with the long-range Coulomb excitation mechanism. Furthermore, we study the consequences of the spreading of the strength distribution of the single giant resonance on the inelastic cross section for both the GR and DGR. These topics have been previously explored in the literature. In refs. (14; 15; 16) nuclear and Coulomb interactions were taken into account for medium-heavy nuclei at low bombarding energy (around 50 MeV/A). While these studies put in evidence interference effects between the two excitation mechanisms there was no clear resolution concerning what could be actually attributed to each of them. Also, the role played by the resonances' width on the reaction cross sections was covered in refs. (17; 18; 13). The analyses, however, were done only for the case of the Coulomb excitation mechanism and lead to somewhat ambiguous results.

We shall do this survey within a simple reaction model that has the virtue of conforming to the standard treatment of inelastic excitations which is familiar to many active participants in this field. Our original intention was limited to investigate the qualitative dependence of the probabilities of excitation of the Double Giant Resonances as a function of several global parameters such as the excitation energies, bombarding energies, multipolarity, anharmonicity, width, etc. In the process of refining the computer programs we used to obtain these global trends we ended up with a quite transparent and yet powerful tool that – we believe – can be useful for the experimentalists to make *quantitative* predictions for measurements in a wide variety of circumstances. With this very practical purpose in mind we shall take in this contribution the width of the states as a free parameter. We shall also limit our calculations to the non-relativistic regime and, for the different examples, consider the excitation of single- and double-phonon Giant Quadrupole Resonances.

Following this Introduction we describe in Sect. II the formalism employed to make our estimates. Relevant results for the reaction  $^{40}\text{Ar} + ^{208}\text{Pb}$  are given with an abundance of illustrations in Sect. III. The conclusions that can be inferred from these examples are also the subject of this Section. Some concluding remarks are left for Sect. IV.

## 2 The Model

The excitation processes of the one and two-phonon states are calculated within the framework of the standard semiclassical model of Alder and Winther (19) for energies below the relativistic limit. According to this model for heavy ion collisions, the nuclei move along a classical trajectory determined by the Coulomb plus nuclear interaction. We will explore the energy range from few MeV up to hundreds of MeV per nucleon. During their classical motion the nuclei are excited as a consequence of the action of the mean field of one nucleus on the other. The excitation processes are described according to quantum mechanics and they are calculated within perturbation theory.

We assume that the colliding nuclei have no structure except for the presence, in the target, of one and two-phonon states whose energies are  $E_1$  and  $E_2 = 2E_1$ , respectively. For the ion-ion potential we have used the Coulomb potential for point charged particles and the Saxon-Woods parametrization of the proximity potential  $U_N(r)$  that are commonly used in heavy ion collisions (20).

In the theory of multiple excitations the set of coupled equations describing the evolution of the amplitudes in the different channels can be solved within the perturbation theory. We can write the probability amplitude to excite the

$\mu$  component of the one-phonon state with multipolarity  $\lambda$  as

$$a_{\lambda\mu}^{(1)}(t) = (-i/\hbar) \int_{-\infty}^{\infty} dt F_{\lambda\mu}(r(t), \hat{r}(t)) e^{iE_1 t/\hbar}, \quad (1)$$

where the integrals are evaluated along the classical trajectories  $\mathbf{r}(t)$ . In this equation the main ingredient is the coupling form factor

$$F_{\lambda\mu}(r(t), \hat{r}(t)) = f_{\lambda}(r) Y_{\lambda\mu}(\hat{r}), \quad (2)$$

chosen according to the standard collective model prescription (21). For a given multipolarity  $\lambda$  the radial part assumes the form

$$f_{\lambda}(r) = \frac{3Z_p Z_t e^2}{(2\lambda + 1)R_C} \beta_{\lambda}^C \left( \frac{R_C}{r} \right)^{\lambda+1} - \beta_{\lambda}^N R_T \frac{d}{dr} U_N(r). \quad (3)$$

The deformation parameters  $\beta$  determine the strength of the couplings, and they are normally directly associated with the  $B(E\lambda)$  transition probability. The expression for the nuclear component of the form factor is not valid for  $\lambda = 1$ . In this case the inelastic form factor is obtained from the Goldhaber-Teller or Jensen-Steinwendel models. The  $Z_p$  ( $Z_t$ ) denotes the charge number of the projectile (target), while  $R_C$  and  $R_T$  are the Coulomb and matter radii of the target nucleus.

In a similar way, the amplitude for populating the two-phonon state with angular momentum  $L$  and projection  $M$  can be obtained as

$$a_{LM}^{(2)}(t) = (1/\hbar)^2 \sum_{\mu} \sqrt{(1 + \delta_{\mu, M-\mu})} \times \int_{-\infty}^{\infty} dt F_{\lambda, M-\mu}(\mathbf{r}(t)) e^{i(E_2 - E_1)t/\hbar} \int_{-\infty}^t dt' F_{\lambda, \mu}(\mathbf{r}(t')) e^{iE_1 t'/\hbar} \quad (4)$$

Solving the classical equation of motion we can calculate for each impact parameter  $b$  the excitation probability  $P^{(1)}(b)$  and  $P^{(2)}(b)$  to populate the single- and the double-phonon state. These are given by

$$P^{(1)}(b) = \sum_{\mu} |a_{\lambda\mu}^{(1)}(t = +\infty)|^2 \quad (5)$$

and

$$P^{(2)}(b) = \sum_L P_L^{(2)} = \sum_{LM} |a_{LM}^{(2)}(t = +\infty)|^2. \quad (6)$$

In order to get the corresponding cross sections we have then to integrate the probabilities  $P^{(\alpha)}$ 's ( $\alpha = 1, 2$ )

$$\sigma_{\alpha} = 2\pi \int_0^{\infty} P^{(\alpha)}(b) T(b) b db. \quad (7)$$

Generally, in Coulomb excitation processes the transmission coefficient is taken equal to a sharp cutoff function  $\theta(b - b_{min})$  and the parameter  $b_{min}$  is chosen in such a way that the nuclear contribution is negligible. We want to take into account also the contribution of the nuclear field so in our case  $T(b)$  should be zero for the values of  $b$  corresponding to inner trajectory and then smoothly going to one in the nuclear surface region. This can be naturally implemented by introducing an imaginary term in the optical potential which describes the absorption due to non elastic channels. Then the survival probability associated with the imaginary potential can be written as

$$T(b) = \exp \left\{ \frac{2}{\hbar} \int_{-\infty}^{+\infty} W(r(t)) dt \right\}, \quad (8)$$

where the integration is done along the classical trajectory. The imaginary part  $W(r)$  of the optical potential was chosen to have the same geometry of the real part with half its depth.

The excitation processes of both single and double GR can change significantly when one takes into account the fact that the strength of the GR is distributed over an energy range of several MeV. Among the few standard choices for the single GR strength distribution, we will assume a Gaussian shape, with a width  $\Gamma_1 = 2.3\sigma$  which we will take as a parameter, of the following form

$$S(E) = \frac{1}{\sqrt{2\pi}\sigma} \exp \left\{ \frac{-(E - E_1)^2}{2\sigma^2} \right\}. \quad (9)$$

Calculations have been also performed with a Breit-Wigner shape yielding similar trends. However, the Gaussian form guarantees a better localization of the response and prevents superposition of the modes for the largest widths (for a further discussion see ref. (5)).

To get the cross section to the one-phonon state one then defines a probability of excitation per unit of energy,

$$dP^{(1)}(E, b)/dE = S(E) \sum_{\mu} |a_{\lambda\mu}^{(1)}(E, t = +\infty)|^2, \quad (10)$$

where the single amplitudes  $a_{\lambda\mu}^{(1)}(E, t)$  are obtained as before, but with a variable energy  $E$ . The probability of exciting the double-phonon state is then obtained by folding the probabilities of single excitation, in the form

$$dP^{(2)}(E, b)/dE = \int dE' \frac{dP^{(1)}(E', b)}{dE} \frac{dP^{(1)}(E - E', b)}{dE} . \quad (11)$$

The total cross section for one- and two-phonon states can then be constructed as

$$\sigma_{\alpha} = 2\pi \int_0^{\infty} \int_0^{\infty} \frac{dP^{\alpha}}{dE}(E, b) T(b) b db dE . \quad (12)$$

Due to the Q-value effect it is clear that one expects a distortion in the shape of the distribution of the cross section which will favor the lower part of the distribution in energy.

### 3 Results

We show in Fig. 1 the dependence on the impact parameter of the excitation probabilities for the one- and two-phonon states of the Giant Quadrupole Resonance in lead. The reaction we have chosen for this illustration is  $^{40}\text{Ar} + ^{208}\text{Pb}$  at a bombarding energy of 40 MeV per nucleon. The deformation parameters have been chosen equal  $\beta^C = \beta^N = 0.07$ , in agreement with the currently estimated value for the  $B(E2)$ . The range of impact parameters given in the figure covers the relevant grazing interval, and in a classical picture (including both Coulomb and nuclear fields) yields scattering angles between 3.4 and 5.5 degrees. In the strictly harmonic case the probabilities for excitation of the double-phonon state can of course be constructed from those corresponding to the single-phonon; they are both explicitly given here for a matter of later convenience. Each frame displays a set of three curves that allows us to compare the individual contributions of the Coulomb and nuclear fields to the excitation process and put in evidence a value of  $b \approx 12.5$  fm for the maximum (destructive) interference between the competing mechanisms.

We use the same reaction as in Fig. 1 to illustrate the effect of the reaction Q-values on the transition probabilities. The dependence of the single-step inelastic excitation to the one-phonon state of energy  $E_{GQR}$  and the sequential process feeding the double-phonon state at twice this value are shown in Fig. 2. As before, the three curves in each frame display the separate contributions

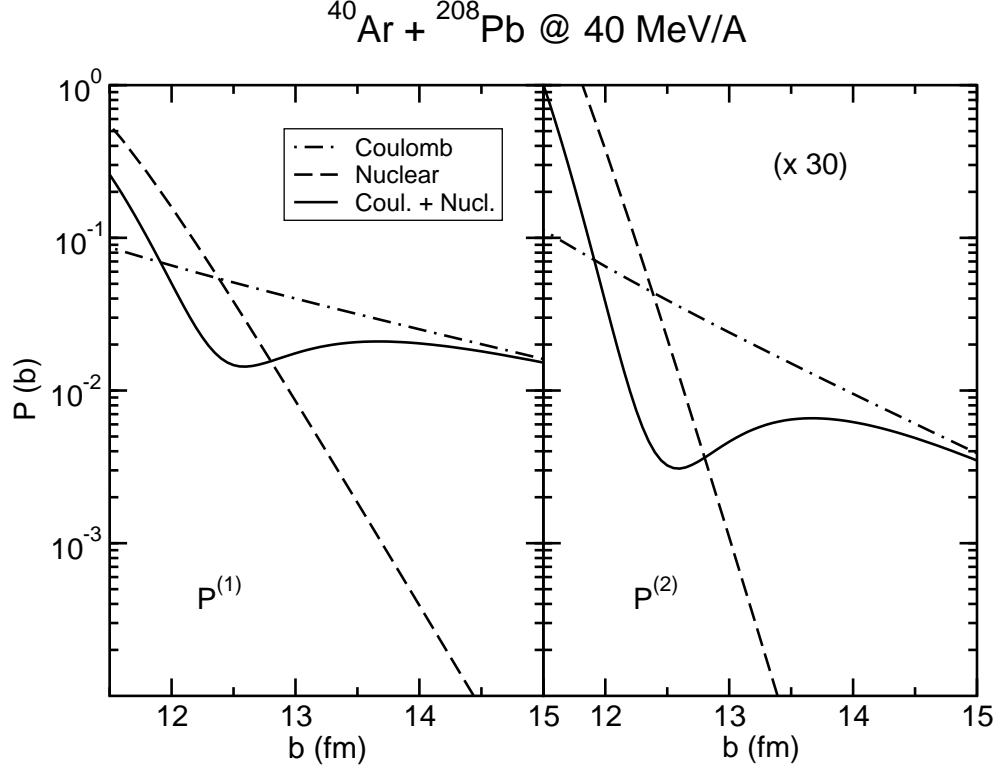


Fig. 1. Excitation probability vs. impact parameter for the one- (left part) and two-phonon (right part) states of the GQR in lead for the reaction  $^{40}\text{Ar} + ^{208}\text{Pb}$  at 40 MeV/A. The Coulomb (dot-dashed line) and nuclear (dashed) probabilities are displayed as well as the total (solid line). The curves on the right part have been multiplied by 30.

of the Coulomb and nuclear fields and the combined total. Two values of the impact parameter have been chosen specifically to cover a situation of nuclear ( $b=12$  fm) and Coulomb ( $b=13$  fm) dominance. The results show – even in a linear scale – a somewhat moderate dependence with the frequency of the mode. This is due to the relatively high bombarding energy chosen in this example, for which the time-dependence of both the Coulomb and nuclear excitation fields are quite well-tuned to the intrinsic response.

There is a qualitative difference in the effective collision time for Coulomb and nuclear inelastic processes that is worth mentioning. We refer to the dependence, for a given bombarding energy, of the excitation probabilities for the one- and two-phonon states on the impact parameter. Because of the long range of the formfactors the change of the effective collision time  $\tau$  for Coulomb excitation follows a different law than the one corresponding to the nuclear inelastic processes. It can be estimated that  $\tau_C/\tau_N \approx A_\lambda \sqrt{b}$ , where the proportionality factor  $A_\lambda$  is a monotonically decreasing function of the multipolarity  $\lambda$ . For all multiplicities, however,  $\tau_C$  is larger than  $\tau_N$ . It follows from these arguments that the adiabatic cut-off function that affects the transition amplitudes for Coulomb excitation varies significantly over the large

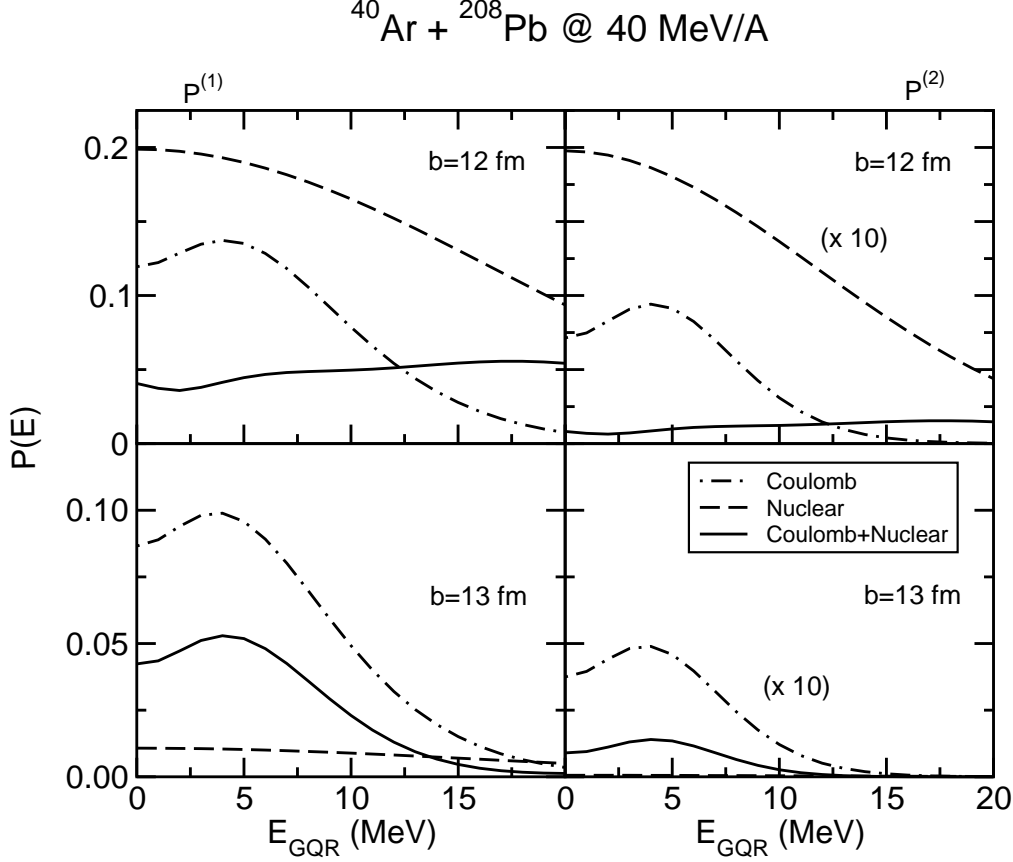


Fig. 2. Excitation probabilities as function of the GQR energy, which is taken as a parameter, for the reaction  $^{40}\text{Ar} + ^{208}\text{Pb}$  at 40 MeV/A. The graphs on the left correspond to the excitation probability of the single GQR ( $P^{(1)}$ ) while the ones on the right correspond to DGQR ( $P^{(2)}$ ) and they are multiplied by a factor 10. The Coulomb (dash-dotted line) and nuclear (dashed) probabilities are displayed as well as the total (solid line). The upper (lower) figures correspond to an impact parameter of 12 (13) fm.

range of impact parameters that contributes to this process. For the nuclear field a favorable matching between effective collision times and the intrinsic period of the mode applies, on the other hand, to most of the relevant partial waves. This can be understood by examining Fig. 3, where the probability for excitation of the one-phonon level is plotted as a function of the energy of the mode for three impact parameters,  $b=10, 15$  and  $20$  fm. Two sets of curves are shown, corresponding to Coulomb and nuclear excitation only. In both instances the probabilities are normalized to their values for  $E_{\text{GQR}}=0$  MeV to emphasize the different character of the response. Notice, for instance, that for  $E_{\text{GQR}}=20$  MeV the role of the Coulomb field for  $b=20$  fm would be effectively quenched by two orders of magnitude in spite of its long range. (This is of course in addition to the gradual reduction of the transition amplitudes caused by the slow  $r^{-(\lambda+1)}$  dependence of the couplings.)



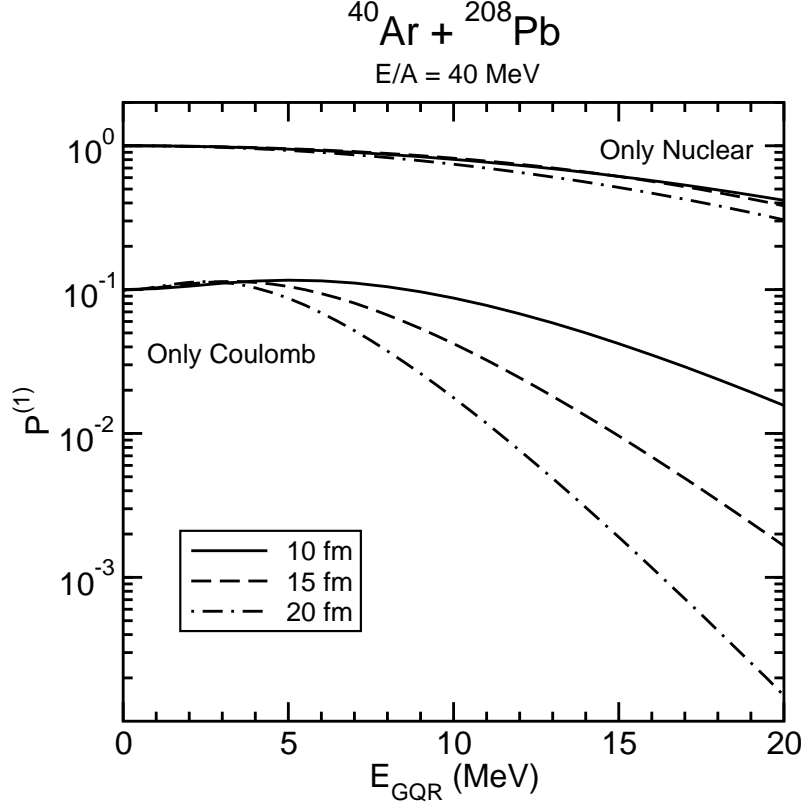


Fig. 3. Excitation probability for the single GQR as a function of the GQR energy for three values of impact parameters. They have been normalized to their values at  $E_{GQR} = 0$ . The upper curves correspond to the excitation probability due only to the nuclear field. The probabilities calculated only with the Coulomb field are shown in the lower part of the picture. They have been divided by 10 in order to render the figure readable.

We use Fig. 4 to illustrate the dependence of the excitation probabilities upon the bombarding energy. For this we take a value of  $E_{GQR} = 11 \text{ MeV}$ , close to the actual excitation energy of the Giant Quadrupole Resonance in lead. The impact parameter  $b$  is set to 12.5 fm, which provides the condition in which the importance of the Coulomb and nuclear excitations become comparable. Of course it is also the choice of impact parameter that yields the maximum (negative) interference between the two reaction mechanisms. What we see is a rapid increase of the probabilities for the one-phonon and two-phonon levels up to a bombarding energy of about 50 MeV/nucleon. After that a gradual decline sets in up to about 400 MeV/nucleon, an energy beyond which a relativistic formalism must be implemented. The trend, however, is not to be significantly altered and, in view of these results one cannot but wonder about the actual need of exploiting relativistic bombarding energies to probe the excitation of double-phonon giant resonances in nuclei. In principle, and entirely from an adiabatic point of view, the higher the bombarding energy the better. Yet, optimal matching conditions reach saturation and one cannot ignore the fact that, beyond this point, one can no longer expect a further enhancement of

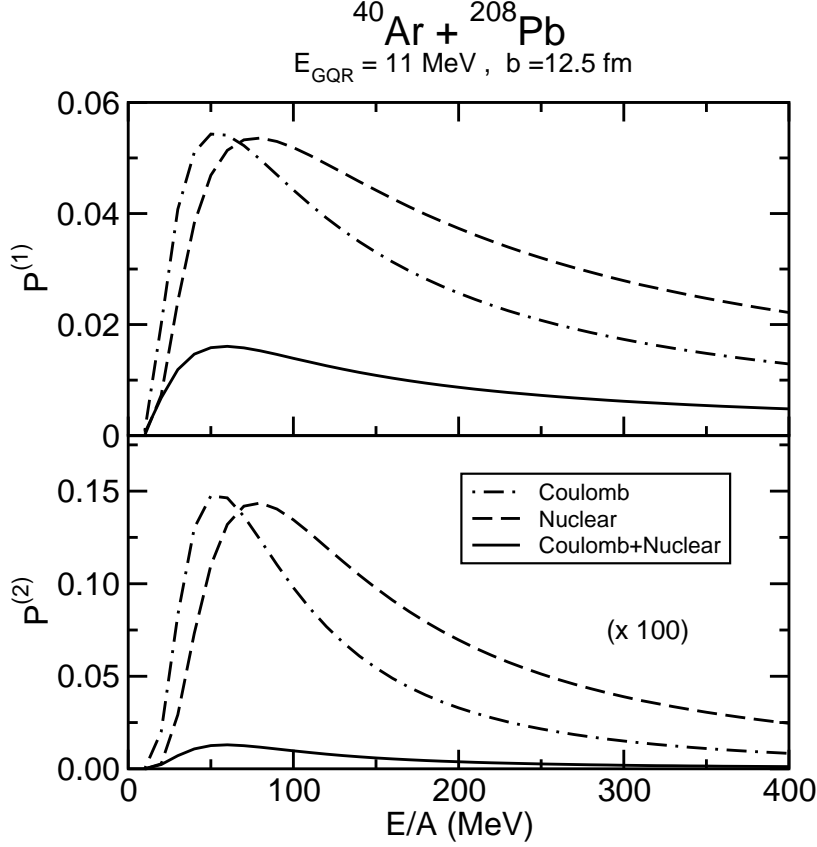


Fig. 4. Excitation probability as a function of incident energy of the one- (upper part) and two-phonon (lower part) states of the GQR in lead for the reaction  $^{40}\text{Ar} + ^{208}\text{Pb}$  for an impact parameter of 12.5 fm. The Coulomb (dot-dashed line) and nuclear (dashed) probabilities are displayed as well as the total one (solid line). The curves on the lower part have been multiplied by 100.

the excitation probabilities. Quite on the contrary, the interaction time is effectively reduced up to a point where (as the figure shows) the excitation of the modes becomes less and less favored (see caption to Fig. 5 and, also, ref. (18)).

In Fig. 6 we display the cross section for the excitation of the GQR and DGQR as a function of the bombarding energy in MeV per nucleon. This observable quantity combines the effect of all impact parameters and the plot puts in evidence a quite interesting feature. Notice that at all bombarding energies the population of the one-phonon state is dominated by the Coulomb formfactors. At the two-phonon level, on the other hand, it is mostly the nuclear coupling that determines the outcome. To understand the origin of this exchange of roles it may be helpful to re-examine Fig. 1. We have here to pay attention to the dependence of the ratio between the probabilities for nuclear and Coulomb excitation in the relevant range of impact parameters, 11-13 fm. (To this end the display factor of 30 introduced for the case of the two-phonon state is of no consequence.) The enhanced logarithmic slopes for

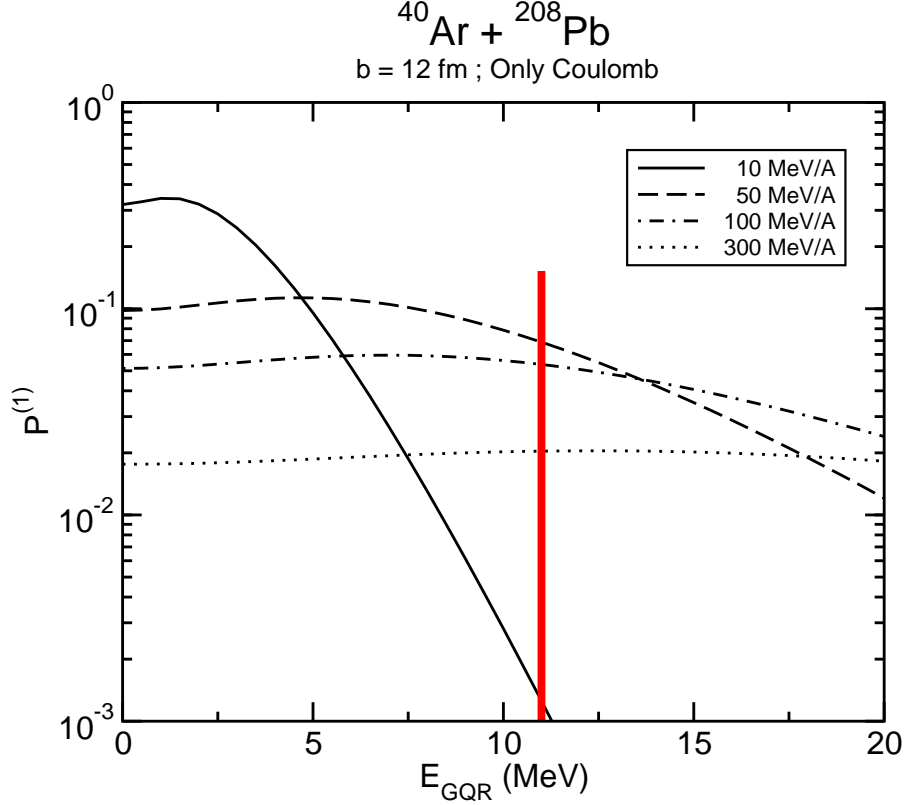


Fig. 5. Coulomb excitation probability for the one-phonon state as a function of the Q-value and for four different incident energies as shown in the legend. The curves correspond to calculations done for an impact parameter  $b=12$  fm. The vertical line indicates the GQR energy for lead.

the DGQR resulting from the squaring of the one-phonon probabilities suffice to give the leading edge to the nuclear couplings. This realization has major consequences insofar as the global properties of the excitation of the GQR and DGQR is concerned. In fact, the transition probabilities will inevitably reflect the different characteristics of the reaction mechanism that it is mostly responsible for the population of one state or the other.

Q-value considerations have such a pronounced effect on the excitation probabilities that it is clear that they will play an important role when one takes into account the sizable width of the one- and two-phonon states. Suppose that instead of having the total strength of the mode at a fixed value  $E_{GQR}$  we distribute it with the profile of a Gaussian distribution of width  $\Gamma$ . If the energy of the mode is quite off the optimal Q-value window one should expect that the distribution of measured cross sections will follow a quite different law. In fact, whenever the dynamic response in the vicinity of  $E_{GQR}$  is a rapidly changing function of the energy (see, for instance, Fig.5 for  $E=10$  MeV/A) the experimental distribution will be significantly distorted and shifted towards lower energies. We illustrate this aspect in Fig. 7, where the distribution of Coulomb excitation probabilities for the one-phonon state,  $dP^{(1)}/dE$ , is shown

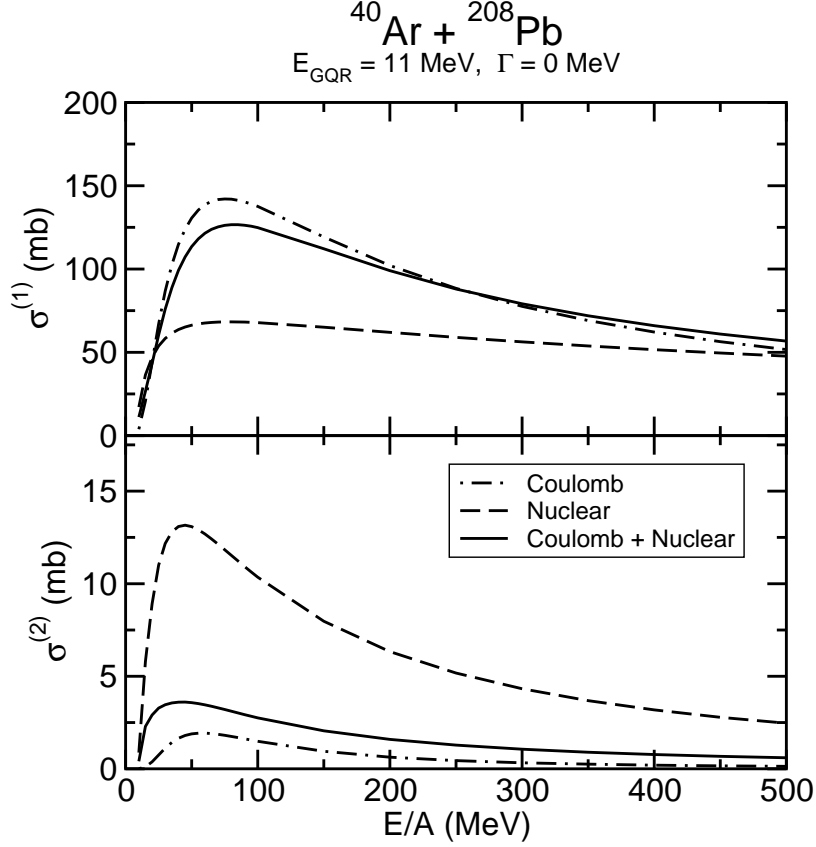


Fig. 6. Excitation cross section for the GQR (upper figure) and DGQR state (lower figure) as a function of the incident energy. Again, the Coulomb (dot-dashed line), nuclear (dashed line) and total (solid line) contributions are shown.

for different impact parameters and bombarding energies. In each frame the shaded curve shows the Gaussian distribution of strength that is the input to the calculation. Notice that all distributions have been normalized in order to emphasize the effect of interest and to eliminate the over-all dependence on  $b$  and  $E$  discussed earlier. As it follows from our considerations one can easily see that the smaller distortion corresponds indeed to the smaller impact parameters and/or the larger bombarding energies.

The distortion of the line profile at the one-phonon level increases as a function of the width  $\Gamma$ , as it is clearly seen in Fig. 8, where reaction cross sections (i.e. the result of an integration over impact parameters) are shown for a typical value of the bombarding energy. For the larger width  $\Gamma=6 \text{ MeV}$  the apparent shift of the distribution is large enough as to place most of the cross section outside of the initial range set by the Gaussian curve. The effect seems to be more noticeable at the two-phonon level, as shown on the right-hand-side of the figure. According to our previous discussion, it is the Coulomb excitation mechanism that contributes most to the difference between the strength and cross section profiles.

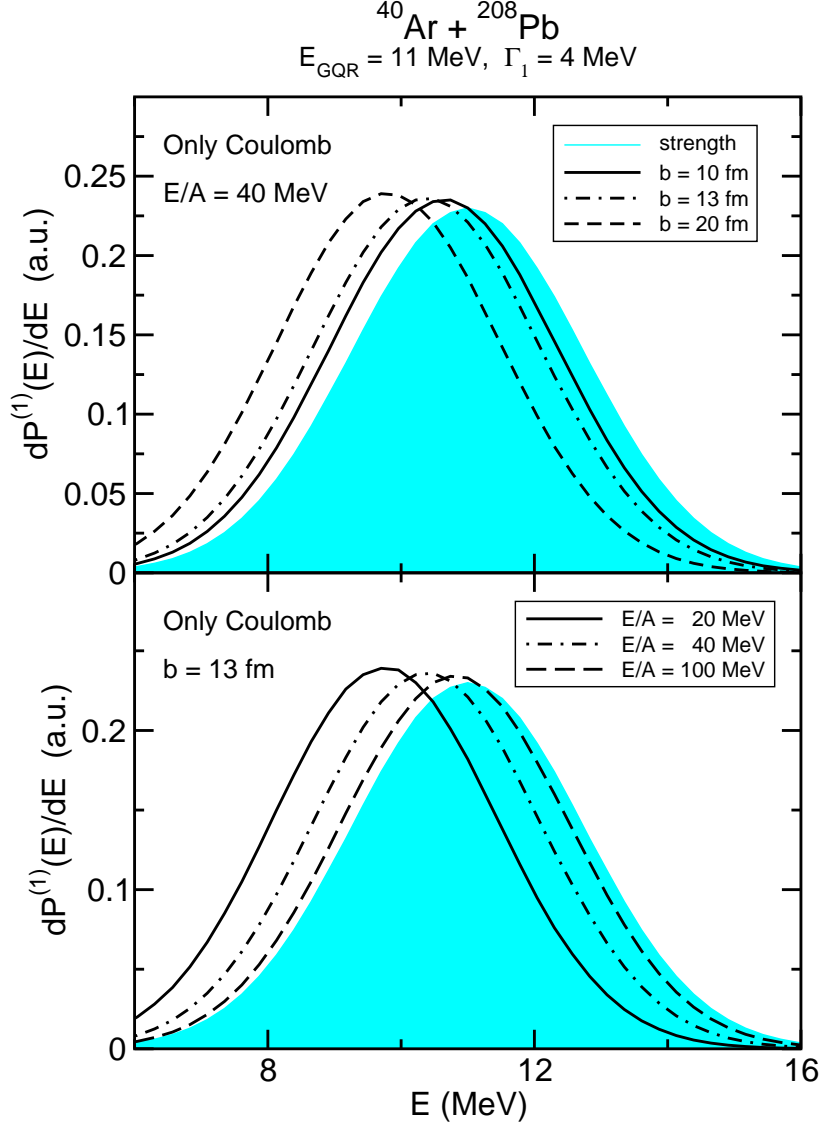


Fig. 7. Normalized distributions of Coulomb excitation probability for the one-phonon state for different impact parameters (upper figure) and bombarding energies (lower figure) as shown in the legend. The shaded area shows the Gaussian strength distribution used as input in the calculation. The width has been chosen to be 4 MeV.

From the energy distributions displayed in Fig. 8 one can calculate the total one- and two-phonon cross sections, by integrating over the excitation energy. The global effect of the finite width is shown in Fig. 9, where the total cross sections for different values of the width are compared with the corresponding values for sharp resonances. The enhanced excitation in the lower part of the distribution leads to a global enhancement in the case of the Coulomb field. As a consequence, a corresponding enhancement is present in the combined Coulomb+nuclear case in the one-phonon excitation, which is dominated by the Coulomb interaction. On the contrary, being the two-phonon cross section

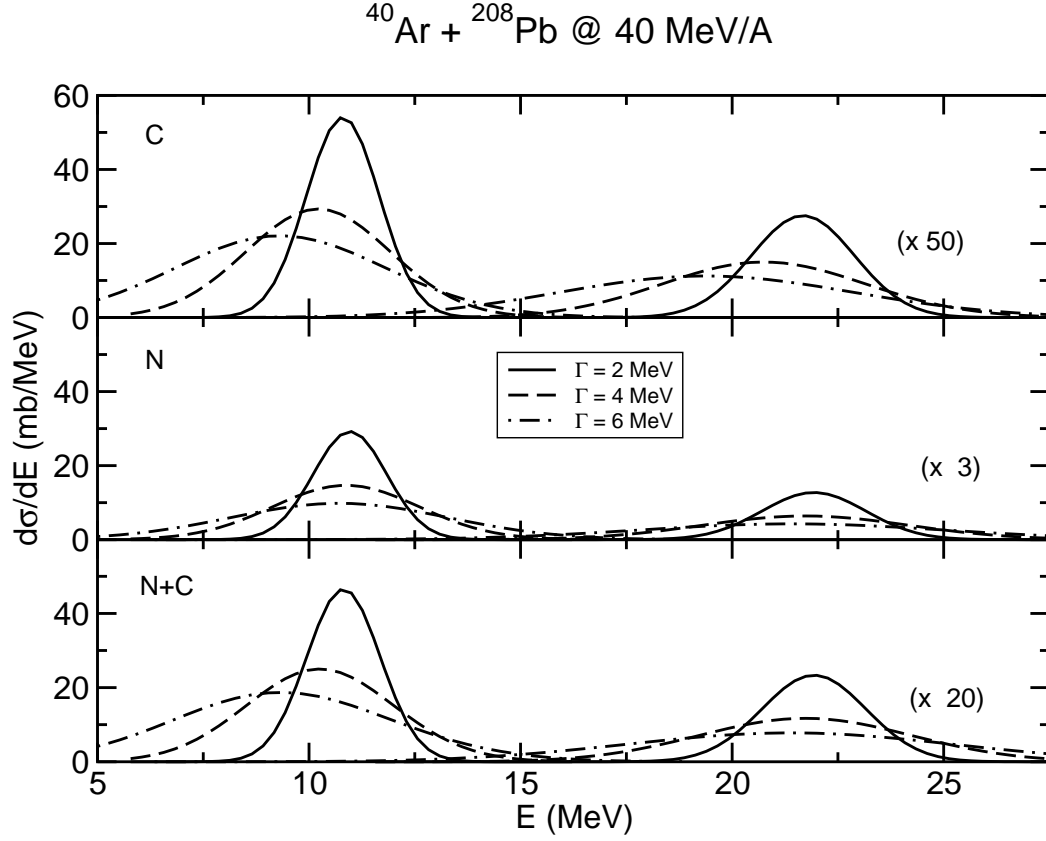


Fig. 8. Cross section distribution for the reaction  $^{40}\text{Ar} + ^{208}\text{Pb}$  at 40 MeV/A for three values of the width as indicated in the legend. The contributions of the Coulomb (C), nuclear (N) and total (N+C) cross sections are shown in single graphs. The cross sections for DGQR are multiplied by the factors reported in the figure.

predominantly due to the nuclear process, no appreciable variation is predicted for this case with finite values of the width.

Since the effect of the width arises from the Q-value kinematic matching conditions, variations are expected with the bombarding energy. In particular one expects that the effects will tend to vanish at high bombarding energies. This is illustrated in Fig. 10, where the total one- and two-phonon cross sections for  $\Gamma = 4 \text{ MeV}$  are compared to the corresponding values for  $\Gamma = 0$  as a function of the incident energy.

#### 4 Conclusions and remarks

We have implemented a simple scheme to calculate the excitation probabilities for the single and double Giant Resonance as a function of several global parameters such as excitation energies, bombarding energies, width etc. We have

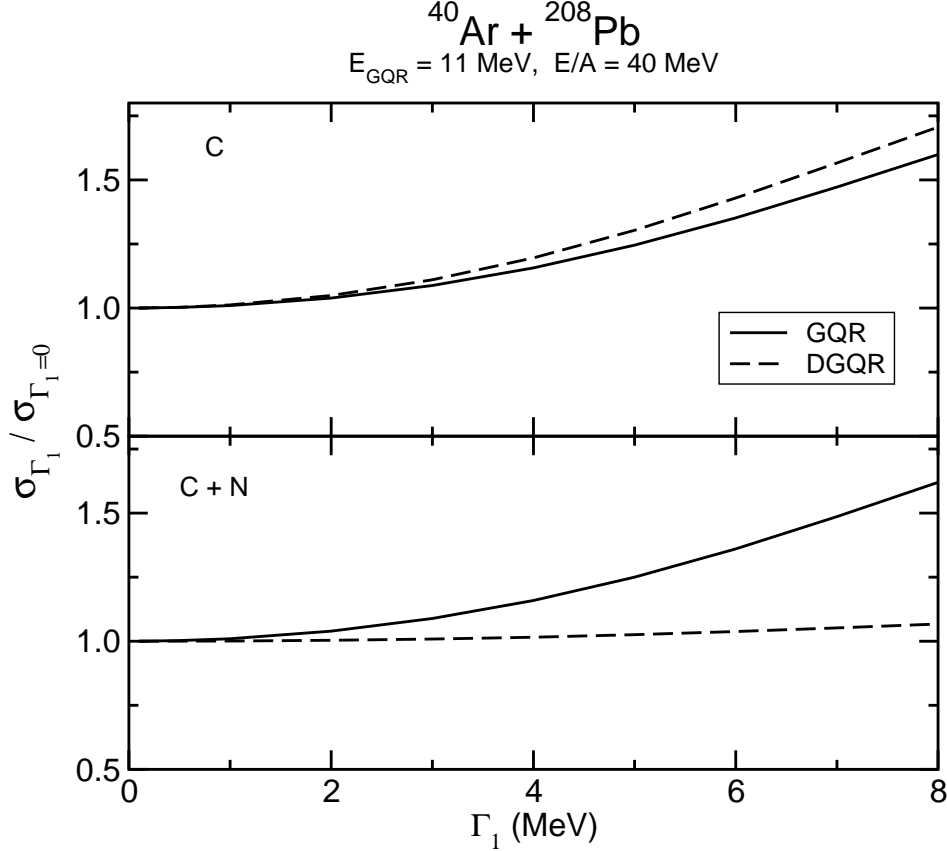


Fig. 9. Total cross sections for the excitation of GQR (solid line) and of DGQR (dashed line) as a function of the strength distribution width  $\Gamma_1$  of the single GQR for the reaction  $^{40}\text{Ar} + ^{208}\text{Pb}$  at  $30 \text{ MeV}/A$ . In the graphs we report the cross sections due to the Coulomb field (upper) and total (lower), each of them divided by their corresponding value for sharp distribution ( $\Gamma_1 = 0$ ). We have not reported the nuclear contribution because the cross sections for both GQR and DGQR do not change appreciably when a finite distribution is assumed.

assumed that the colliding nuclei have no structure except for the presence, in the target, of one and two-phonon states. The excitation processes have been calculated within a semiclassical model and according to perturbation theory. Since both nuclear and Coulomb interaction are taken into account the cross sections are calculated by integrating over all range of impact parameter with an imaginary potential that takes care of the inner trajectories. The formalism has been applied to the excitation of giant resonances in a typical heavy ion reaction,  $^{40}\text{Ar} + ^{208}\text{Pb}$ . In our examples, we have limited our calculation to the giant quadrupole resonance.

The role of the nuclear interaction and its interplay with the long-ranged Coulomb field has been studied. The presence of nuclear coupling modifies the mechanism excitation of both the GR and the DGR, the effect being strongly evident in the latter. This has been ascribed to the difference in the

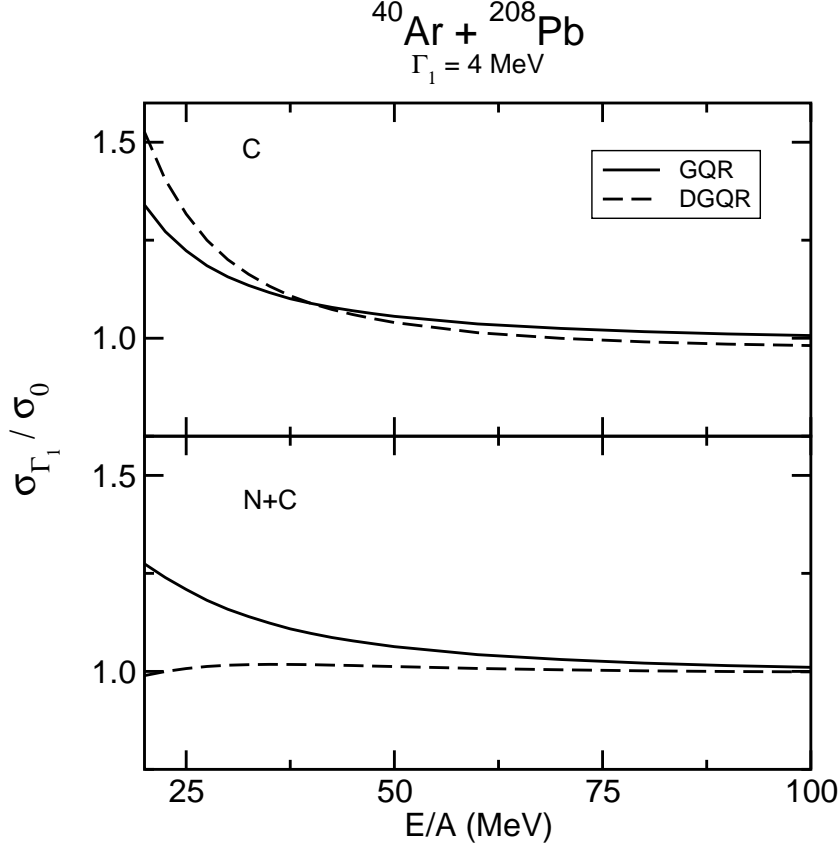


Fig. 10. Same as fig. 9 as a function of the bombarding energy. The strength distribution width has been chosen equal to 4 MeV.

effective collision time which, together with the qualitative  $r$  dependence of the form factors, produces a different dependence of the transition probabilities on the reaction Q-value. Hence, the excitation of GR is dominated by the Coulomb interaction while it is mostly the nuclear coupling which determines the population of the DGR.

We have also studied the consequences of the spreading of the strength distribution of the single giant resonance on the inelastic excitation of the GR and DGR. Q-value considerations play an important role when the width of the one- and two-phonon states are considered. Cross section dependence on both the width of the distribution and the incident energy has been considered. When compared with the corresponding values for sharp resonances, the cross sections for GR and DGR calculated with only the Coulomb field increase as  $\Gamma$  increases. These results are qualitatively similar to the one obtained in ref. (13) where the relativistic Coulomb excitation of dipole giant resonance (GDR) and double GDR are calculated within a random matrix theory including the Brink-Axel hypothesis. When the nuclear interaction is switched on, the enhancement for the single GR is maintained while the two-phonon cross section presents no variation with the case of finite value of the width. Also



for the dependence on the incident energies has been found the same trend. This is due to the fact that the two-phonon cross section is predominantly governed by nuclear processes.

## 5 Acknowledgment

This work has been partially supported by the Spanish-Italian agreement between CICyT and INFN and by the Italian MIUR under contract PRIM 2001-2003 *Fisica teorica del nucleo e dei sistemi a molti corpi*.

## References

- [1] M. N. Harakeh and A. van Woude, *Giant Resonances* (2001 Oxford University Press, New York).
- [2] H. Hemling, Prog. Part. Nucl. Phys. **33** (1994) 729; Ph. Chomaz, and N. Francaria, Phys. Rep. **252** (1995) 275; T. Aumann, P. Bortignon, and H. Emling, Annu. Rev. Part. Sci. vol. **48** (1998) 351.
- [3] S. Nishizaki and J. Wambach, Phys. Lett. **B349** (1995) 7; Phys. Rev **C57** (1998) 1515.
- [4] V. Yu. Ponomarev, P. F. Bortignon, R. A. Broglia, E. Vigezzi and V. V. Voronov, Nucl. Phys. **A599** (1996) 341c.
- [5] C. A. Bertulani and V. Yu. Ponomarev, Phys. Rep. **321** (1999) 139.
- [6] F. Catara, Ph. Chomaz and N. Van Giai, Phys. Lett **B233** (1989) 6.
- [7] V. Yu. Ponomarev, P. F. Bortignon, R. A. Broglia, and V. V. Voronov, Phys. Rev. Lett. **85** (2000) 1400.
- [8] E. G. Lanza, M. V. Andrés, F. Catara, Ph. Chomaz and C. Volpe, Nucl. Phys. **A613** (1996) 445; Nucl. Phys. **A654** (1999) 792c.
- [9] C. Volpe, F. Catara, Ph. Chomaz, M. V. Andrés and E. G. Lanza, Nucl. Phys. **A589** (1995) 521; Nucl. Phys. **A599** (1996) 347c.
- [10] P. F. Bortignon and C. H. Dasso, Phys. Rev. **C56** (1997) 574.
- [11] D. Brink, PhD Thesis, Oxford University, 1955, unpublished; P. Axel, Phys. Rev. **126** (1962) 671.
- [12] B. V. Carlson et al., Ann. Phys. (NY) **276** (1999) 111; Phys. Rev. **C60** (1999) 014604.
- [13] J. Z. Gu and H. A. Weidenmüller, Nucl. Phys. **A690** (2001) 382.
- [14] F. Catara, Ph. Chomaz and A. Vitturi, Nucl. Phys. **A471** (1987) 661.
- [15] E. G. Lanza, M. V. Andrés, F. Catara, Ph. Chomaz and C. Volpe, Nucl. Phys. **A636** (1998) 452.
- [16] M. V. Andrés, F. Catara, E. G. Lanza, Ph. Chomaz, M. Fallot and J. A. Scarpaci, Phys. Rev **C65** (2001) 014608.

- [17] L. F. Canto, A. Romanelli, M. S. Hussein and A. F. R. de Toledo Piza, Phys. Rev. Lett. **72** (1994) 2147.
- [18] C. A. Bertulani, L. F. Canto, M. S. Hussein and A. F. R. de Toledo Piza, Phys. Rev. **C53** (1996) 334.
- [19] K. Alder and A. Winther, *Electromagnetic Excitation* (North-Holland, Amsterdam, 1975).
- [20] R. A. Broglia and A. Winther, *Heavy Ion Reactions* Vol.I (1981 The Benjamin/Cummings Publishing Company).
- [21] S. Landowne and A. Vitturi, in *Treatise on Heavy Ion Science*, Ed. D. A. Bromley, vol. 1, p.355.